Extended Cavitands of Nanoscale Dimensions

Edoardo Menozzi,[a] Hideki Onagi,[a] Arnold L. Rheingold,[b] and Julius Rebek, Jr.*[a]

Keywords: Supramolecular chemistry / Cavitands / Host-guest systems

New tetrabenzimidazole cavitands with upper rims extended by aromatic groups have been prepared and their X-ray structures were analyzed. The reversible encapsulation of a series of *n*-alkylammonium guests was studied by NMR spectroscopy and mass spectrometry. These guests showed different binding modes and unique interactions with the hydrophobic cavity. The trimethylammonium guests bearing *n*-butyl to *n*-hexyl substituents stabilize the C_{4v} conformation of the cavitand by additional CH···π interactions with the aromatic upper part. The longest *n*-hexylammonium salt adopts a minimal *gauche* conformation to fit in the cavity.

Cavitands are open-ended host molecules possessing enforced cavities in which complementary guest molecules can be accommodated.[1] Most are derived from shallow resorcinarenes that are deepened through synthesis, but such changes can also result in conformations that no longer possess well-defined cavities.[2] Additional features such as a cyclic array of intramolecular hydrogen bonds,[3] and even covalent bonds can stabilize a vase-like structure. These allow the formation of kinetically stable complexes with sizeable guests like adamantane derivatives[4] and ammonium cations.[5] We report here the synthesis and characterization of three new tetrabenzimizadole cavitands with upper rims extended by aromatic groups. The binding of a series of alkylammonium salts is analyzed by NMR methods that show idiosyncratic behavior of the cations in filling the space of the hosts.

The synthesis (Scheme 1) proceeds from the known resorcinarenes **1a**,**b** and follows well-trodden paths. Two different alkyl chains were deployed at the lower rim of resorcinarene: To improve the solubility in organic media we used R = $C_{11}H_{23}$; to favor the formation of crystals for X-ray determination we used R = C_2H_5. The octanitro derivatives **2a**,**b** were prepared by alkylation of **1a**,**b** with 4 equiv. of 4,5-difluoro-1,2-dinitrobenzene, then reduction using $SnCl_2$ in EtOH/HCl, and subsequent base workup gave **3a**,**b**. The extended walls were installed by the treatment of the octamines **3a** or **3b** with an excess of the appropriate aldehyde using the benzimidazole ring formation protocol described by Singh et al.[6] Accordingly, the very upper rim of the cavitands can be basic (**4a**,**b**), neutral (**5**) or functional (**6**). Cavitands **4**–**6** were obtained in 20–30% yield and were characterized by NMR spectroscopy and mass spectrometry. A crystal of the cavitand **5** was obtained by slow diffusion of EtOH into its solution in CH_2Cl_2. The crystal structure shows that the cavitand has a deep vase-like conformation (Figure 1, Table 1), stabilized by four EtOH molecules that form a network of hydrogen bonds with the benzimidazole rings. The cavity is filled with two additional molecules of EtOH, one deep inside the cavity while the second one is located between the phenyl and imidazole region. The distance between the methine carbon atom and the *para* position of the corresponding phenyl group is 12.1 Å; the width is 7–8 Å, and the approximate volume of 300 Å^3 makes this one of the largest cavitands known that can be used for the inclusion of long alkyl ammonium salts. The X-ray structure of **4a** was also obtained and showed nearly identical features (for Supporting information see footnote on the first page of this article).

Trimethylammonium salts from *n*-C_2H_5 to *n*-C_6H_{13} and cavitand **5** form kinetically stable 1:1 inclusion complexes on the NMR time scale in [D_6]DMSO (Table 1). The electron-rich aromatic surfaces of the hosts provide cation–π attractions[7] with the partially positive hydrogen atoms on the surface of the guests. ESI-MS clearly shows that only one guest molecule is contained in the gas phase as well (prominent peaks at [(**Guest@5**)-Br]$^+$ and [(**Guest@5**)+Na]$^+$; **Guest** refers to compounds **7**–**11**).

The NMR spectra of the included guests are shown in Figure 2. The shorter guests **7** and **8** show signals broadened by exchange with their free counterparts with a rate that, at the temperature employed for the experiments, is still slower but not very different than the ^{1}H NMR chemical shift time scale (600 MHz). Relatively sharp signals are seen for complexes with guests *n*-C_4H_9 to *n*-C_6H_{13} (**9**–**11**)

[a] The Skaggs Institute for Chemical Biology and Department of Chemistry, The Scripps Research Institute, MB-26,
10550 North Torrey Pines Road, La Jolla, California 92037, USA
E-mail: jrebek@scripps.edu
[b] Department of Chemistry and Biochemistry, University of California at San Diego,
La Jolla, California 92093, USA

Supporting information for this article is available on the WWW under http://www.eurjoc.org or from the author.

 DOI: 10.1002/ejoc.200500342

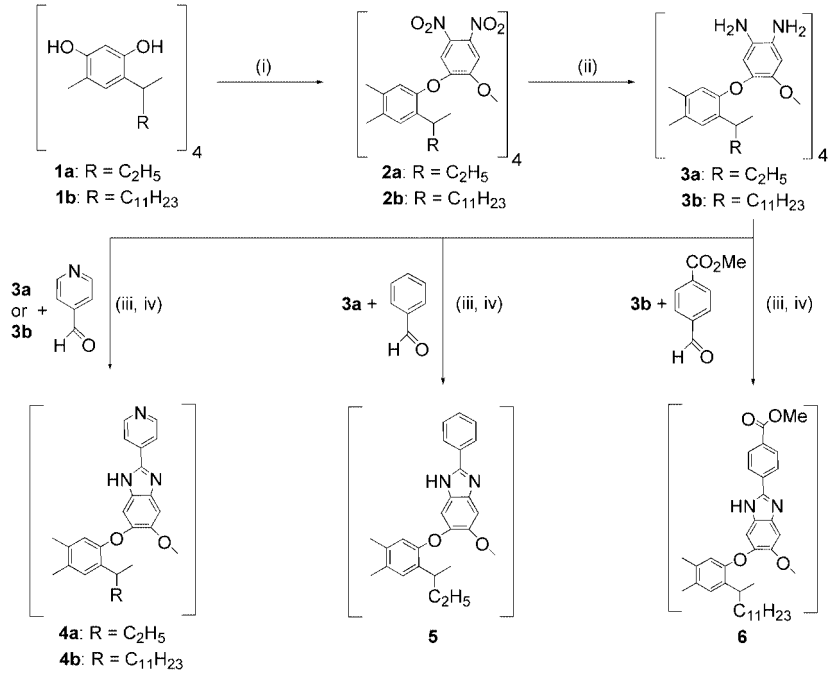

Scheme 1. Synthesis of the tetraimidazole-modified cavitands **4**–**6**. i) 4,5-difluoro-1,2-dinitrobenzene, DMF, 70 °C, 16 h; ii) $SnCl_2$, EtOH/HCl, 70 °C, 16 h followed by base workup; iii) DMF, 80 °C, 2 h, under N_2; iv) $FeCl_3{\cdot}6H_2O$, DMF, 110 °C, 16 h.

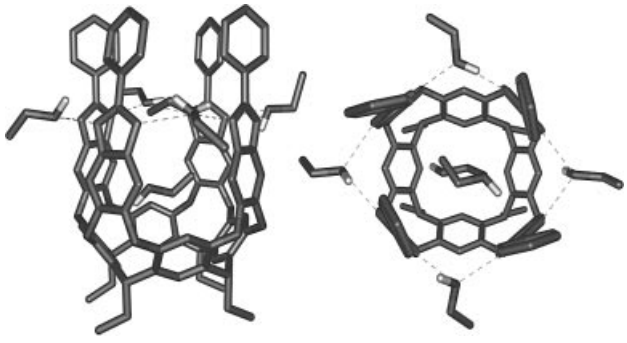

Figure 1. X-ray structure of cavitand **5** crystallized from CH_2Cl_2/EtOH.

and separate signals are observed for each methylene and for the terminal methyl group. The longer guests **9**–**11** stabilize the C_{4v} conformation of the cavitand: The ^1H NMR spectra of the complexes are sharper than the free host's spectrum. The chemical shifts of each methylene and methyl group were assigned by 2D-COSY experiments (see Supporting information). These exposed some unusual features. For example, the trimethylammonium groups (NMe_3) of **9**–**11** are deeply buried in the cavity and are subjected to maximal upfield shifts with $\Delta\delta$ up to –5.0 ppm. Not so with the shortest compound **7**. Here the methyl group of the ethyl group is directed at the tapered end and shows the furthest upfield shift. Also, the signal of the terminal CH_3 group of the *n*-hexyl group of **11** appears at δ = –1.21 ppm, while the signals of the terminal methyl groups of the butyl and pentyl compounds are found at δ = –2.26 ppm. This difference in the chemical shift in the case of **11** places it almost out of the cavity, but where? The behavior of these guests is summarized as follows. The *n*-butyl compound **9** is the most straightforward to interpret and will be used as a reference. The magnetic shielding provided by the aromatic rings of the hosts is greatest near the tapered bottom

Table 1. Crystal data and structure refinement for **5**. High values of *R* and *wR* are due to disordered solvent molecules present in the unit cell.

Empirical formula	$C_{100}H_{96}N_8O_{14}$
Formula mass	1633.85
Temperature	120(2) K
Wavelength	0.71073 Å
Crystal system	triclinic
Space group	$P\bar{1}$
Unit cell dimensions	a = 15.394(3) Å; α = 110.556(3)°
	b = 15.540(3) Å; β = 92.603(3)°
	c = 19.781(4) Å; γ = 92.784(3)°
Volume	4415.6(14) Å^3
Z	2
Density (calculated)	1.229 g/cm^3
Absorption coefficient	0.083 mm^{-1}
F(000)	1728
Crystal size	0.40×0.05×0.03 mm
θ range for data collection	1.40–27.53°
Index ranges	$-19 \le h \le 20$, $-20 \le k \le 20$,
	$-24 \le l \le 25$
Reflections collected	37008
Independent reflections	19098 [R(int) = 0.0857]
Completeness to θ	θ = 27.53°; 93.9%
Absorption correction	none
Max./min. transmission	0.9975/0.9677
Refinement method	full-matrix least-squares on F^2
Data/restraints/parameters	19098/0/1099
Goodness-of-fit on F^2	1.134
Final R indices [$I > 2\sigma$(I)]	R_1 = 0.1552, wR_2 = 0.2981
R indices (all data)	R_1 = 0.2598, wR_2 = 0.3345
Largest difference peak/hole	0.709/–0.373 e·Å^{-3}

of the cavitand; it gradually decreases near the imidazole region of the cavitand then increases at the top near the four phenyl groups. This trend gives some predictability; the chemical shifts report the positions of the hydrogen atoms in the cavity (Figure 3). The trimethylammonium group, *t* ($\Delta\delta$ = –5.0 ppm) is deepest, then the proximal methylene group *a* [signal at δ = –1.2 ppm ($\Delta\delta$ = –4.5 ppm)]. Next deepest is the *b* methylene group [signal found at δ = –2.2 ppm ($\Delta\delta$ = –3.8 ppm)]. The sheer, *tert*-butyl-like bulk of the trimethylammonium group insures that the conformation around the *a*–*b* bond is *trans*-antiperiplanar; in this extended conformation the signal of the hydrogen atoms at the *c* position appears at δ = –1.5 ppm ($\Delta\delta$ = –2.7 ppm). Modeling (Figure 3) places the *c* methylene group at about the midpoint of the single bond that connects the phenyl groups to the benzimidazole groups, i. e. in a magnetic environment less shielded than positions below and, as we shall soon see, above. The *a*, *b*, *c* and *t* signals of **9**–**11** are fairly constant but a slight downfield drift is apparent with increasing size. This indicates that the longer guests **10** and **11** are not quite as deep in the cavity as the shorter one **9**. The signal for the terminal methyl group of **9** at δ = –2.2 ppm is also shifted ($\Delta\delta$ = –2.8 ppm) and places it in the center of the deshielding regions of the four phenyl groups. Accordingly, the butyl group of **9** is in a maximally extended conformation.

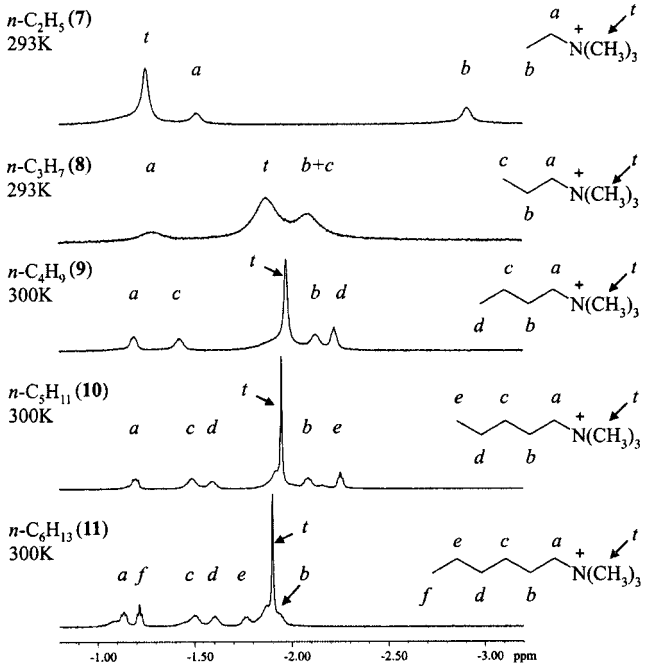

Figure 2. Up-field regions of the ^{1}H NMR spectra at 600 MHz in [D_6]DMSO of encapsulated alkylammonium bromide salts at [**5**] = 2 mM, [guest] = 10–15 mM. Broad peaks close to signals *t* arise from different arrangements of hydrogen bonds in cavitand **5**, which cause a slight modification of the shielding effect in the cavity.

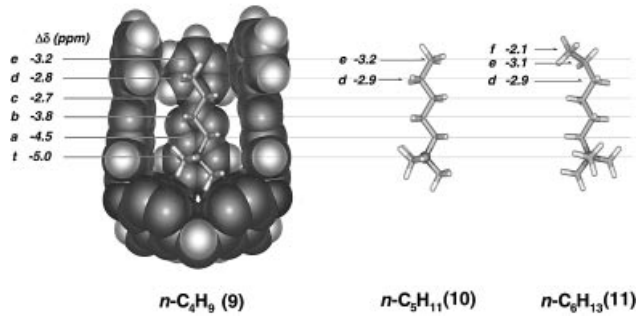

Figure 3. Energy-minimized structures of the inclusion complex between cavitand **5** and *n*-alkylammonium guests **9**–**11** (MMFF force field); one wall of the receptor has been removed for viewing clarity. Gradient of the shielding effect inside cavitand **5** is shown.

We already mentioned that the very short compound **7** presents its ethyl group toward the bottom of the cavity (note the positions of the trimethylammonium and terminal methyl signals). The broadened spectrum of **8** speaks for another dynamic process of intermediate rate on the NMR timescale and that appears to be tumbling. For **8**, it was not possible to detect separate signals for each methylene group and for the terminal methyl group, even though the ^{1}H NMR was recorded at 293 K. This is supported by the position of the signals for *b* and *c* at $\delta \approx$ –2.1 ppm. The *c* signal of **8** is considerably upfield of its counterparts, fixed in space in complexes of **9**, **10** and **11**. Tumbling of these longer alkyl salts is improbable, but they are expected to rotate freely about the longitudinal axis of the cavitand. The case of *n*-C_5H_{11} (**10**) also appears fully extended although its terminal methyl signal *e* appears at the same chemical shift as that of the shorter but fully extended compound **9**. The downfield shift of signal *d* ($\Delta\delta$ = 0.6 ppm) is comparable to what happens outside the capsules for methyl vs. methylene group. For the *n*-C_6H_{13} group of **11** the terminal methyl group *f* is in a minimally shielding environment. At first glance, this would place it beyond the upper rim of the cavitand, a position it could achieve in a fully extended conformation. The signal for *e* has also moved downfield ($\Delta\delta$ = 0.5 ppm) as before. A *gauche* interaction about the *d*–*e* bond reconciles the chemical shifts and places the ter-

Table 2. Data of the trimethylammonium salts included in cavitand **5**.

	Length [Å]	Volume [Å^3]	*PC*[a]	K_{ass} [M^{-1}]	ESI-TOF [*m*/*z*]
n-$C_2H_5N(CH_3)_3Br$ (**7**)	5.6	106	0.35	90 ± 30	[**7**@**5**-Br]$^+$ = 1449.6 [**7**@**5**+H]$^+$ = 1526.5
n-$C_3H_7N(CH_3)_3Br$ (**8**)	6.8	122	0.41	110 ± 50	[**8**@**5**-Br]$^+$ = 1463.6 [**8**@**5**+Na]$^+$ = 1564.7
n-$C_4H_9N(CH_3)_3Br$ (**9**)	8.1	140	0.46	370 ± 50	[**9**@**5**-Br]$^+$ = 1477.6 [**9**@**5**+Na]$^+$ = 1578.5
n-$C_5H_{11}N(CH_3)_3Br$ (**10**)	9.4	153	0.51	550 ± 50	[**10**@**5**-Br]$^+$ = 1491.6 [**10**@**5**+Na]$^+$ = 1592.5
n-$C_6H_{13}N(CH_3)_3Br$ (**11**)	10.6	172	0.57	230 ± 80	[**11**@**5**-Br]$^+$ = 1505.6 [**11**@**5**+Na]$^+$ = 1606.5

[a] *PC*: Packing coefficient.

minal methyl group between two adjacent phenyl groups rather than near the center of the cavitand. This is shown on the right in Figure 3.

The relative affinities of the guests were obtained from NMR titrations (Table 2) and a direct competition experiment between *n*-C_5H_{11} (**10**) and *n*-C_6H_{13} (**11**) shows the former to be the better guest (Figure 4). The difference in binding free energies is calculated to be ca. 0.5 kcal/mol, a value near the energetic cost of a single *gauche* interaction (0.5–0.6 kcal/mol in the liquid phase).[8] As the C–H···π interactions, the surface areas of **10** and **11**, their packing coefficients (PC)[9] and positioning also differ, this difference in energies is likely a coincidence.

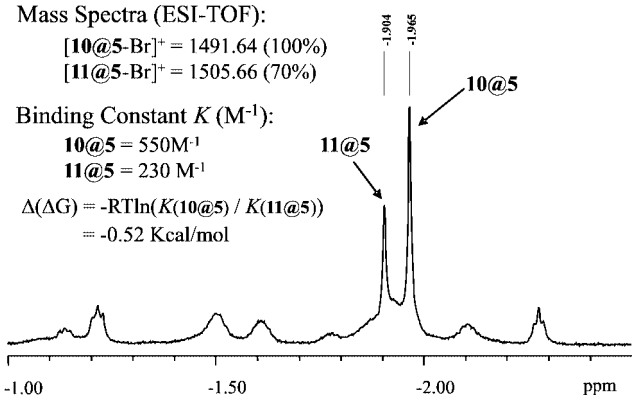

Figure 4. Competition experiment between guests *n*-pentyl/*n*-hexyltrimethylammonium bromide, ^{1}H NMR ([D_6]DMSO) and ESI-TOF data are reported.

Extensive conformational changes involving coiling of long alkyl chains in cavitands and capsules has been previously encountered.[10] In the cases at hand the *gauche* conformation is supported by 2D-NOESY experiment (see Supporting information) that is consistent with the conclusions regarding the positions of the guests in the cavitand. What is unexpected concerns the variation of binding modes in a seemingly simple homologous series: almost every guest shows a unique interaction with the host. These deeper, functionalizable cavitands promise increasing capacities for reactions between host and guest or even between two guests.

Supporting Information (see footnote on the first page of this article): Synthetic procedures and spectroscopic data of cavitands **4**–**6**; 2D NMR spectra of inclusion complexes; X-ray crystallographic data of the cavitand **4a** (CCDC-277575 contains the supplementary crystallographic data for this paper. These data can be obtained free of charge from The Cambridge Crystallographic Data Centre via www.ccdc.cam.ac.uk/data_request/cif).

Acknowledgments

We are grateful to the Skaggs Institute and the National Institutes of Health for financial support. E. M. and H. O. are Skaggs Postdoctoral Fellows.

[1] Reviews: a) D. J. Cram, J. M. Cram, in: *Container Molecules and Their Guests* (Ed.: F. Stoddart), The Royal Society of Chemistry, Cambridge, London, **1994**; b) P. Timmerman, W. Verboom, D. N. Reinhoudt, *Tetrahedron* **1996**, *52*, 2663–2704; c) D. M. Rudkevich, J. Rebek, Jr., *Eur. J. Org. Chem.* **1999**, 1991–2005; d) Z. Asfari, V. Böhmer, J. Harrowfield, J. Vicens, M. Saadioui, *Calixarenes*, Kluwer Academic Publishers, Dordrecht, Netherlands, **2001**.
[2] D. J. Cram, H.-J. Choi, J. A. Bryant, C. B. Knobler, *J. Am. Chem. Soc.* **1992**, *114*, 7748–7765.
[3] a) D. M. Rudkevich, G. Hilmersson, J. Rebek, Jr., *J. Am. Chem. Soc.* **1998**, *120*, 12216–12225; b) T. Haino, D. M. Rudkevich, A. Shivanyuk, K. Rissanen, J. Rebek, Jr., *Chem. Eur. J.* **2000**, *6*, 3797–3805; c) S. Saito, C. Nuckolls, J. Rebek, Jr., *J. Am. Chem. Soc.* **2000**, *122*, 9628–9630.
[4] L. D. Corinne, C. L. D. Gibb, E. D. Stevens, B. C. Gibb, *J. Am. Chem. Soc.* **2001**, *123*, 5849–5850.
[5] a) A. F. Far, A. Shivanyuk, J. Rebek, Jr., *J. Am. Chem. Soc.* **2002**, *124*, 2854–2855; b) S. M. Biros, E. C. Ullrich, F. Hof, L. Trembleau, J. Rebek, Jr., *J. Am. Chem. Soc.* **2004**, *126*, 2870–2876.
[6] M. P. Sing, P. S. Malvinder, S. Sasmal, W. Lu, N. C. Manashi, *Synthesis* **2000**, *10*, 1380–1390.
[7] D. A. Dougherty, *Science* **1996**, *271*, 163–168.
[8] E. Eliel, S. H. Wilen, *Stereochemistry of organic compounds*, Wiley, New York, **1994**.
[9] S. Mecozzi, J. Rebek, Jr., *Chem. Eur. J.* **1998**, *4*, 1016–1022.
[10] a) L. Trembleau, J. Rebek, Jr., *Science* **2003**, *301*, 1219–1220; b) A. Scarso, L. Trembleau, J. Rebek, Jr., *Angew. Chem. Int. Ed.* **2003**, *42*, 5499–5502; c) A. Scarso, L. Trembleau, J. Rebek, Jr., *J. Am. Chem. Soc.* **2004**, *126*, 13512–13518; d) B. W. Purse, J. Rebek, Jr., *Chem. Commun.* **2005**, 722–724.

Received: May 11, 2005
Published Online: July 20, 2005

